IFSCC 2025 full paper (IFSCC2025-1105)

"The relationship between mitochondrial metabolic abnormalities in aging cells and wrinkles in the dermis revealed by Photothermal Microscopy"

Airi Ikeda* [1], Sho Iguchi[1], Satoshi Dozen[1], Hideki Iwano[1], Yohsuke Hada[1], Koji Okamoto[2], Shigetoyo Sawaki[1]*

[1] Life Science General Institute, Technoble Co., Ltd.,; [2] Graduate School of Frontier Biosciences, Osaka University, Osaka, Japan

1. Introduction

The formation of wrinkles is primarily caused by reduced collagen and elastin production in the dermis, which leads to sagging skin. This reduction in production is driven by factors such as UV rays and aging. [1] Collagen, a vital protein in our body, provides structure to the skin, tendons, ligaments, and bones. [2] Its synthesis is a complex process that requires various cellular components and energy sources, particularly ATP (adenosine triphosphate). ATP is the primary energy currency of the cell, and it plays a crucial role in numerous biochemical processes, including collagen synthesis. The synthesis of collagen involves several stages, and ATP is essential at multiple steps. During collagen production, the process begins with the transcription of collagen genes into messenger RNA (mRNA) in the cell nucleus. The mRNA is then translated into preprocollagen, a precursor of collagen, in the ribosomes. Preprocollagen undergoes several post-translational modifications to become functional collagen. These modifications include hydroxylation, glycosylation, and the formation of triple helices. Hydroxylation, in particular, requires the enzyme prolyl hydroxylase, which depends on ATP for its activity. [3] After modifications, the collagen precursors are transported to the Golgi apparatus for further processing and then secreted into the extracellular matrix. [4] The transport and secretion of these molecules are ATP-dependent processes, as vesicular transport systems require energy to move cargo within the cell and across the cell membrane. In the extracellular matrix, collagen molecules assemble into fibrils, which then cross-link to form robust collagen fibers. [5] This assembly and cross-linking process also depend on ATP, as energy is required to facilitate the interactions between collagen molecules and other matrix components. The synthesis of collagen is a highly energy-dependent process, with ATP playing a critical role at every step. Understanding the relationship between ATP and collagen synthesis is essential for developing strategies to enhance collagen production, which is vital for maintaining healthy skin and connective tissues. As we age, the efficiency of ATP production and collagen synthesis declines, leading to the appearance of wrinkles and other signs of aging. [6] By targeting ATP production pathways and ensuring adequate energy supply, it may be possible to boost collagen synthesis and promote healthier, more youthful skin. Cellular aging negatively

impacts mitochondria, leading to reduced ATP synthesis. As mitochondria degrade, the efficiency of energy production falls, resulting in less ATP, which is essential for various cellular processes, including collagen synthesis, contributing to aging signs like wrinkles. We used Photothermal microscopy (PTM) to investigate how aging affects mitochondria in dermal cells because PTM allows us to visualize mitochondrial activity and structure changes without labels, providing insights into age-related cellular dysfunction and potential anti-aging strategies.

2. Materials and Methods

Cell

We used NB1RGB (RIKEN, Japan) and NHDF (KURABO, Japan). These were cultured with Eagle's MEM (SHIMADZU, Japan) supplemented with 10% Newborn Calf Serum (ThermoFisher Scientific, USA) @37℃ and 5.0% CO_2.

Population Doubling Level

Cells were detached with trypsin, collected in Eargle's MEM containing 10% NCS, and counted. 9.0 x 10^4 cells were seeded in 6-well plate and the rest were suspended in ISOGEN II. This was repeated and PDL was calculated from the counted cell count. [7]

Real-Time PCR

Cells were seeded in 6-well plates (9.0×10^4 cells/well) in Eagle's MEM medium containing 0.5% NCS and cultured for 1 week. The cells were collected with 0.5 mL of ISOGEN Ⅱ reagent (Nipon gene, Japan). The recovered total RNA was subjected to reverse transcription reaction using the prescribed kit (PrimeScript RT reagent Kit with gDNA Eraser, TAKARA BIO, Japan), and cDNA was synthesized. All genes were measured by using Thermal Cycler Dice Real Time System Single with SYBR Premix Ex TaqTM2 (TAKARA BIO, Japan). The test results were compared with the expression of each gene in each test section when the expression of the ACTB gene was kept constant.

Photothermal Microscopy imaging

The cells were irradiated with laser light consisting of pump and probe light of different wavelengths, and the reaction in which light absorption energy is converted into heat at cytochromes in mitochondria was detected by a photodetector as an electrical signal. The signals detected by the detector were then extracted and quantified using Image J. [8] Only the portions of the signal that appeared as a tube shape were extracted and quantified.

Mitochondrial membrane potential staining

Cells were seeded in Eagle's MEM medium containing 0.5% NCS and cultured for 2 ~ 7 days. The supernatant was removed and MT-1 (DOJINDO, # MT13) diluted 1000-fold in Eagle's MEM medium containing 0.5% NCS was added and incubated at 37℃, 5% CO_2 for 30 min. After washing twice with PBS, 15% Formalin Neutral Buffer Solution (Wako, Japan) was added and incubated for 30 min at room temperature. After removing the supernatant and washing with PBS, Hoechst 33342 (Wako, Japan) diluted 1000-fold in PBS was added and sealed with an inclusion agent.

Immunofluorescence Staining

Cells were seeded in slide and chamber 4-well coated collagen (5.0×10^4 cells/well) in Eagle's MEM medium containing 0.5% NCS and cultured for 2 ~ 7 days. If plant extracts were added, additions were made the day after seeding. After completion of incubation, the supernatant was removed and washed twice with PBS and placed in 15% neutral buffered formalin solution

for 30 minutes at room temperature. After fixation, the cells were washed twice with PBS and shaken in PBS containing 0.5% Triton-X100 (Nacalai tesque, Japan) at room temperature for 1 hour, and then shaken in Blocking solution (1% BSA/0.1% Tween20/PBS) for 1 hour. Primary antibodies (anti-TOMM20(GENETEX, GNT-GTX133756-100), anti-α tubulin(Proteintech, # 11224-1-AP), vimentin(Cosmo Bio, # 22031-1-AP)) were diluted 500~1000 fold in blocking solution and allowed to stand for 1 hour (room temperature) or overnight (4°C). For staining of actin filaments, 100 nM Phalloidin (Cytoskelton, # PHDR1) was used. After removing the supernatant, the cells were washed 5 times with PBS containing 0.5% Triton-X100 for 5 minutes, and then permeabilized by adding secondary antibody (Alexa Fluor 546 Goat Anti-rabbit IgG (Invitrogen, # A-11010)) and shading at room temperature for 2 hours. Staining of actin filaments was excluded processing of secondary antibodies. After removing the supernatant, the cells were washed 5 times with PBS containing 0.5% Triton-X100 for 5 minutes, the encapsulant was added and encapsulated.

MTT assay

Cells were seeded in 96-well plates (1.0×10^4 cells/well) in Eagle's MEM medium containing 0.5% NCS and cultured for 1 day. Next day, plant extracts are added and incubated for 3 days. After completion of incubation, the medium was removed and Hoechst33342 diluted 1000-fold in PBS was added and incubated at 37℃ and 5% CO_2 for 30 minutes, and fluorescence values were measured at Em=355 nm and Ex=460 nm with a fluorescence plate reader. Next, 0.03% MTT/PBS was added and maintained at 37℃ for 1 hour, purified formazan was extracted with isopropanol, and MTT values were measured at 570~630 nm wavelength using a microplate reader (ThermoFisher Scientific, # Multiskan FC).

Collagen production

Cells were seeded in 96-well plates (1.0×10^4 cells/well) in Eagle's MEM medium containing 0.5% NCS and cultured for 1 day. Next day, plant extracts are added and incubated for 5 days. The medium was removed, the cells were fixed with cold methanol (Wako, # 134-01833) and cold ethanol, and then stained with 0.1% Sirius Red saturated picric acid solution. After washing with purified water, extraction was performed in 0.1% NaOH (Wako, # 192-15985) : methanol = 1:1 solution, and the amount of collagen was measured at 540 nm wavelength using a microplate reader (ThermoFisher Scientific, # Multiskan FC).

Elastin production

Cells were seeded in 96-well plates (1.0×10^4 cells/well) in Eagle's MEM medium containing 0.5% NCS and cultured for 1 day. Next day, plant extracts are added and incubated for 5 days and the medium was changed on day 7. Plant extracts were made the day after seeding. After completion of incubation, the supernatant was removed and washed with PBS and placed in 10% trichloroacetic acid (Nacalai tesque, # 34603-15) for 30 minutes at 4℃. After fixation, the cells were washed with PBS and shaken in PBS containing 0.2% Triton-X100 at room temperature for 1 hour, and then shaken in 5 fold diluted Blocking One-P (Nacalai tesque, # 05999) for overnight (4°C). After removing the supernatant, Primary antibodies (anti-elastin (Merck Millipore, # MAB2503)) were diluted 100 fold in blocking solution and allowed to stand for overnight (4°C). After removing the supernatant, the cells were washed 5 times with PBS containing 0.2% Triton-X100 for 3 minutes, and then permeabilized by adding secondary antibody (Alexa Fluor 546 Goat Anti-rabbit IgG) and shading at room temperature for 2 hours. After removing the supernatant, the cells were washed 5 times with PBS containing 0.2% Triton-X100 for 5 minutes, fluorescence values were measured at Em=544 nm and Ex=590 nm with a fluorescence plate reader.

3. Results

3.1 Senescent HDFs decreased rate of proliferation and produced less extracellular matrix.

Fibroblasts extracted from adults showed a decline in proliferation speed with repeated passages. Notably, there was a significant decrease in growth rate between the 20th and 30th passages, and almost no proliferation occurred between the 30th and 40th passages (Figure 1a). Total RNA was harvested at each passage, and the expression levels of p21 were compared, showing a significant increase after the 20th passage (Figure 1b). This confirmed the successful induction of cellular aging using fibroblasts. Additionally, it was observed that the cells became flattened due to aging.

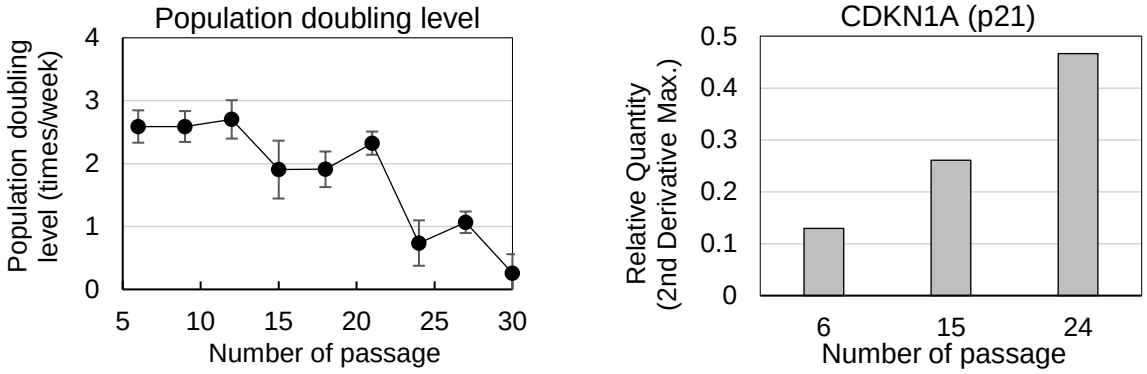

(**a**) (**b**)

Figure 1. The Hallmark of SASP (senescence-associated secretory phenotype) increase with passage aging in HDFs. **;** (a) The population doubling level of human dermal fibroblasts (HDFs) between 6-30th passages. (b) Expression levels of CDKN1A (p21) from the 6th to 24th passages of HDFs by RT-qPCR.

Comparing collagen synthesis levels (Figure 2a) and elastin synthesis levels (Figure 2b) between normal HDFs (number of passage before 20th passages) and senescent HDFs (number of passage after 25th passages), both were found to decrease due to aging. This reconfirmed that aging leads to a decline in the extracellular matrix.

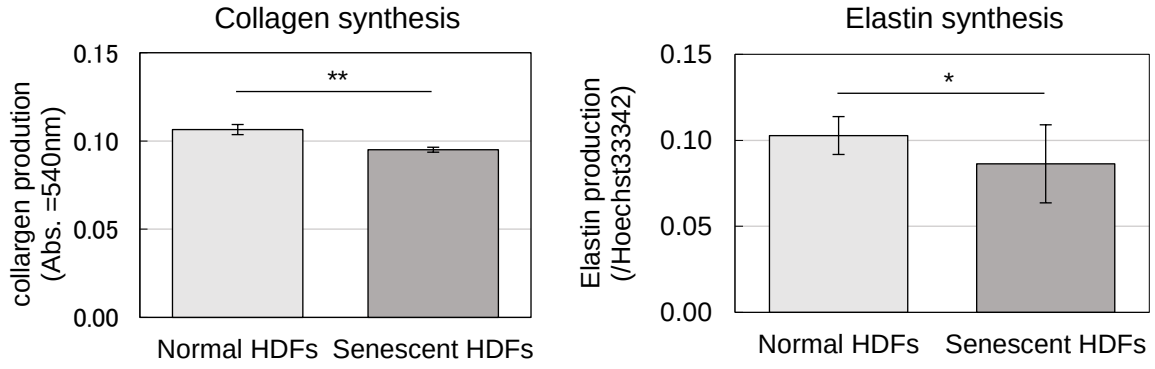

(**a**) (**b**)

Figure 2. Collagen and elastin production decreased in aging HDFs. ; (a) The amount of intracellular collagen fiber of normal and senescent HDFs. (b) Graph shows normal and senescent HDFs immunostained with anti-elastin antibody. The amount of elastin per DNA which is stained with Hoechst 33342.

3.2 PT signals detected by Photothermal microscopy are new aging biomarker that can be observed in living cells.

Photothermal microscopy is a label-free technique that detects refractive index changes caused by light absorption in a sample. [9] It uses two beams of different colors to visualize cellular components such as mitochondria, enabling insights into cellular functions without fluorescent markers (Figure 3, Miyazak and Toumon (2019). Biomed opt express, 10(11), 5852–5861. Figure 1 [9]).

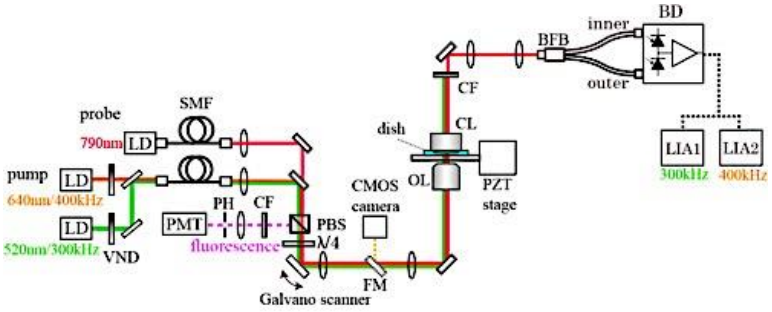

Figure 3. Schematic of the experimental setup. LD, laser diode; SMF, single-mode fiber; PBS, polarizing beam splitter; CF, color filter; PH, pinhole; PMT, photomultiplier tube; FM, flip mirror; OL, objective lens; CL; collection lens; BFB, bifurcated fiber bundle; BD, balanced detector; LIA, lock-in amplifier. Miyazak *and Toumon* (2019). Biomed opt express, 10(11), 5852–5861. [9]

When observing normal HDFs and senescent HDFs using photothermal microscopy, PT signal weakening was confirmed in aged fibroblasts, as shown in Figure 4a. Particularly, when quantifying signals around the nucleus using Image J, a decrease was observed (Figure 4b).

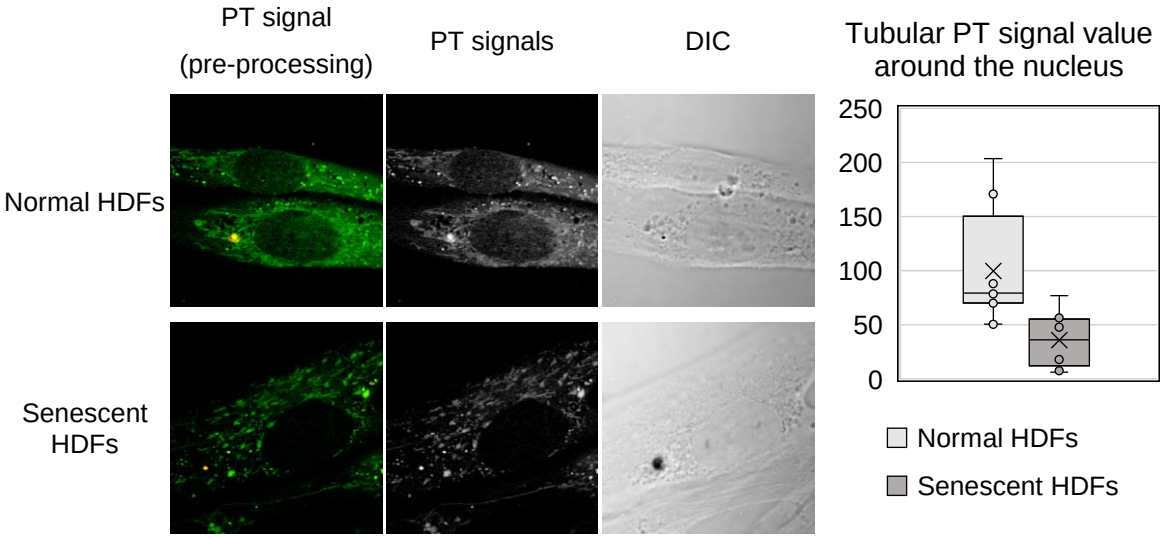

Figure 4. PT signals of senescent HDFs decrease compared with normal human dermal fibroblasts. ; (a) Normal HDFs and senescent HDFs were fixed with 15% formalin for 30 min at room temperature. The left panels were a typical example taken with a PT microscopy. The central panels were edited images taken with a PT microscopy. The right panels were photographed using a phase contrast microscope. (b) PT signal value around the nucleus using image J.

Next, we compared the expression levels of TOMM20, which is localized on the mitochondrial membrane, and found no significant changes in mRNA and protein between normal HDFs and senescent HDFs (Figures 5a). However, when observed with photothermal microscopy, signal weakening was confirmed in senescent HDFs (Figures 5b). Additionally, using the MT-1 reagent, we visualized the mitochondrial membrane potential and observed it simultaneously with photothermal microscopy, showing a correlation between the signals of the two (Figure 5c).

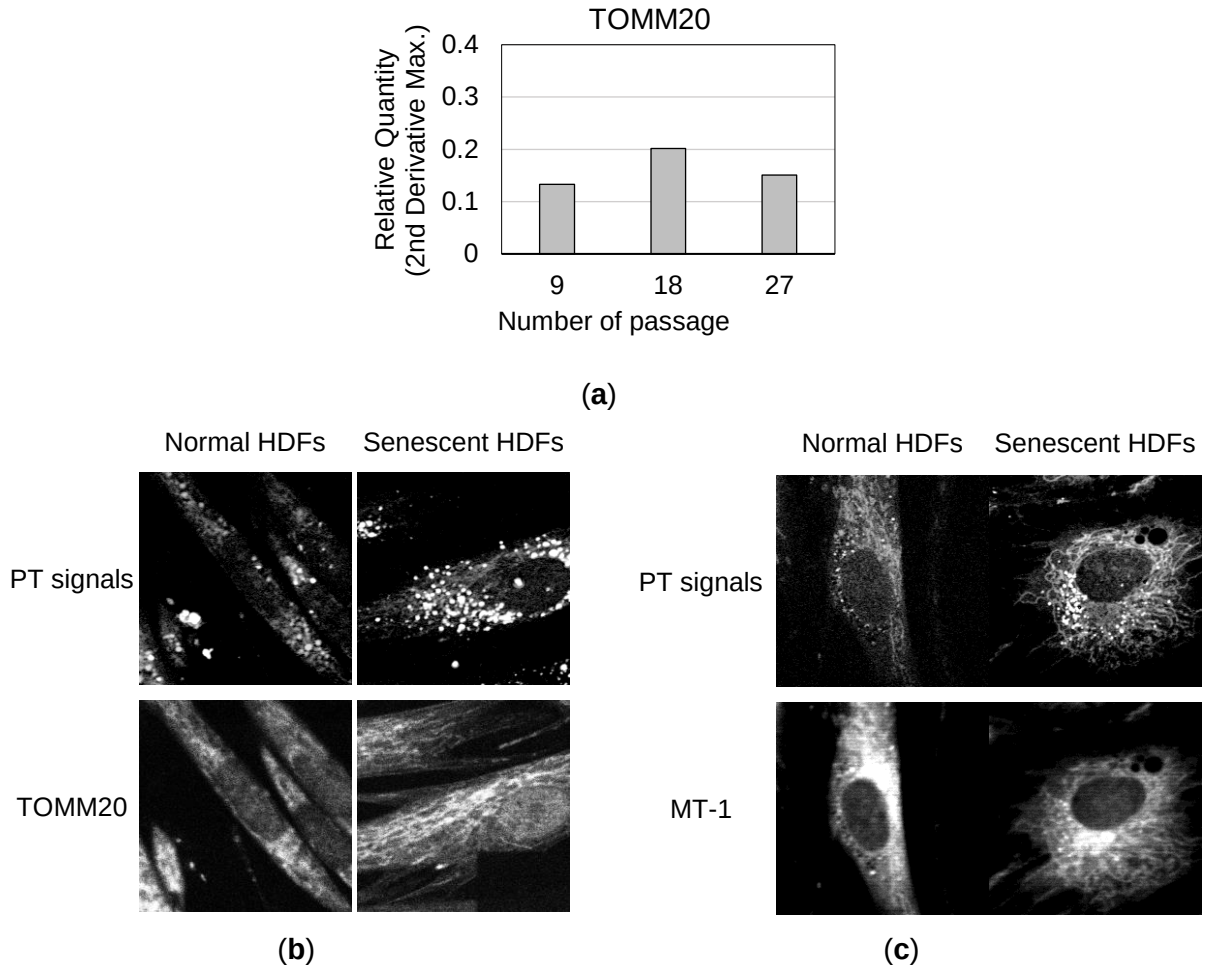

Figure 5. The amount of TOMM20 which is localized on mitochondrial membrane didn't change at each passage, but mitochondrial membrane potential was decreased during aging. ; (a) Expression levels of TOMM20 from the 9th to 27th passages of HDFs by RT-qPCR. (b) Normal HDFs and senescent HDFs were taken with the PT signals (upper) and immunostained with anti-TOMM20 antibody of the same samples (lower). (c) Normal HDFs and senescent HDFs were taken with the PT signals (upper) and stained with MT-1 (lower)

3.3 We discover natural ingredient that increased PT signals in senescent HDFs.

When senescent HDFs were treated with various plant extracts and observed using photothermal microscopy, some extracts were found to enhance PT signals and fluoresence of MT-1 (Figure 6a). Additionally, these extracts were also confirmed to increase MTT activity (Figure 6b). Particularly, in extract C with high MTT values, the cell morphology changed from flat to fibrous.

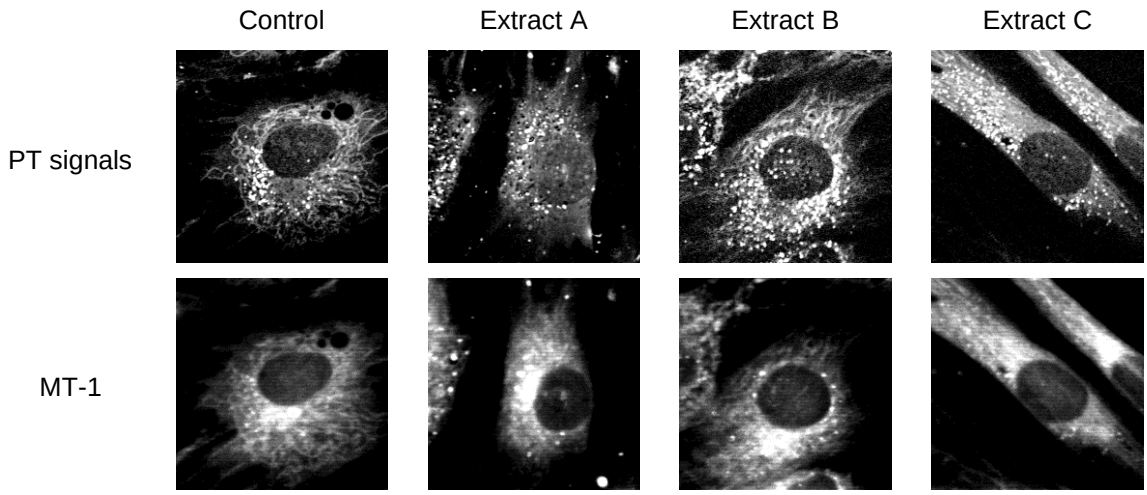

(**a**)

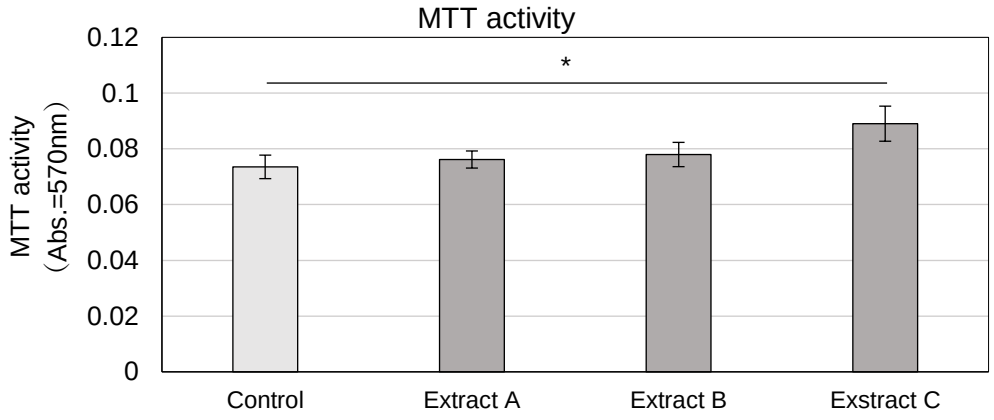

(**b**)

Figure 6. Some plant extracts could increase PT signals and MT-1 in senescent HDFs.; (a) Senescent HDFs with or without some plant extracts were fixed with 15% formalin for 30 min at room temperature. (b) MTT assay for the senescent HDFs with or without some plant extracts.

It has been reported that mitochondria are localized with the cytoskeleton, and the major cytoskeletal structures—microtubules, F-actin and intermediate filament—were visualized by immunostaining (Figure 7). [10] Localization of microtubules seemed to correlated with PT signals, but not with F-actin. Also, intermediate filament it could not be stained well.

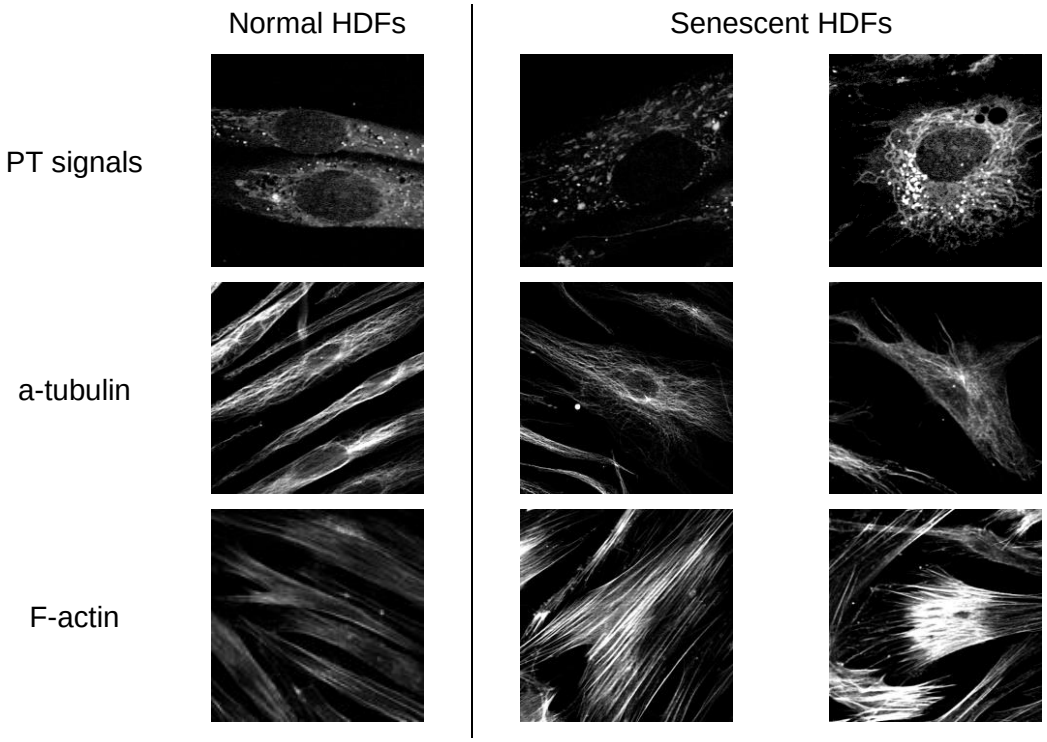

Figure 7. The most significant changes in cytoskeleton were observed in microtubules during aging.Normal HDFs and senescent HDFs were fixed with 15% formalin for 30 min at room temperature. They were stained with anti-α-tubulin and phalloidin for Immunohistochemistry.

Finally, the cosmetic effects of each plant extract were confirmed. When each extract was added to aged fibroblasts and the collagen synthesis levels and elastin synthesis levels were compared, extracts B and C both showed an increase (Figure 8).

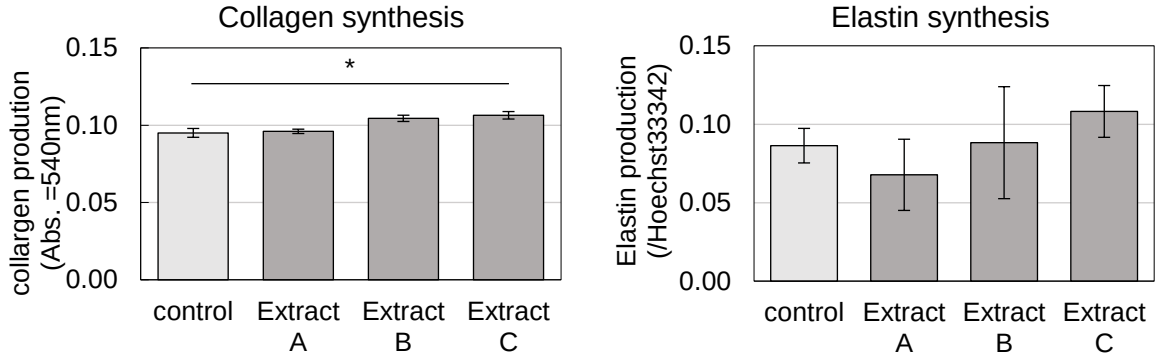

(**a**) (**b**)

Figure 8. Plant extract increased collagen and elastin production in senescent HDFs. ; (a) The amount of intracellular collagen fiber of senescent HDFs with or without some plant extracts. (b) Graph shows normal and senescent HDFs immunostained with anti-elastin antibody. The amount of elastin per DNA which is stained with Hoechst 33342.

4. Discussion

Through observations using photothermal microscopy, the following findings were established when comparing normal HDFs and senescent HDFs across five parameters: mitochondrial quantity, membrane potential, cytoskeleton (microtubules, F-actin), and MTT activity. With

aging, PT signals decrease, and mitochondrial membrane potential declines. Additionally, the microtubules, which constitute the cytoskeleton, exhibit a disrupted morphology. There is a correlation among fibroblasts' aging, PT signals, membrane potential, and microtubule phenotype. On the other hand, no correlation was found with mitochondrial quantity or other cytoskeletal components. Furthermore, several plant extracts were confirmed to increase PT signal. Not only the PT signal but also changes in cell morphology were observed. It was confirmed that the increase in PT signals by plant extracts led to an increase in extracellular matrix components such as collagen and elastin.

5. Conclusion

Based on the results of this study, the following can be inferred: as cells age, the mitochondrial membrane potential decreases, leading to a reduction in ATP production. This decrease in ATP production subsequently causes abnormalities in the maintenance of microtubules. Microtubules are essential components of the cytoskeleton, providing structural support and shape to cells. They play a crucial role in cell division by forming the mitotic spindle, which segregates chromosomes during mitosis. Additionally, microtubules are involved in intracellular transport, serving as tracks for the movement of organelles and vesicles via motor proteins like kinesin and dynein. They also contribute to cell motility by forming cilia and flagella, enabling cells to move and interact with their environment. Overall, microtubules are vital for maintaining cell integrity, facilitating transport, and ensuring proper cell division. Photothermal microscopy has been shown to be useful both as an indicator of cellular aging and in the search for natural components with anti-aging effects. In the near future, as the world faces an aging society, photothermal microscopy will play a significant role in the development of products with anti-wrinkles effects.

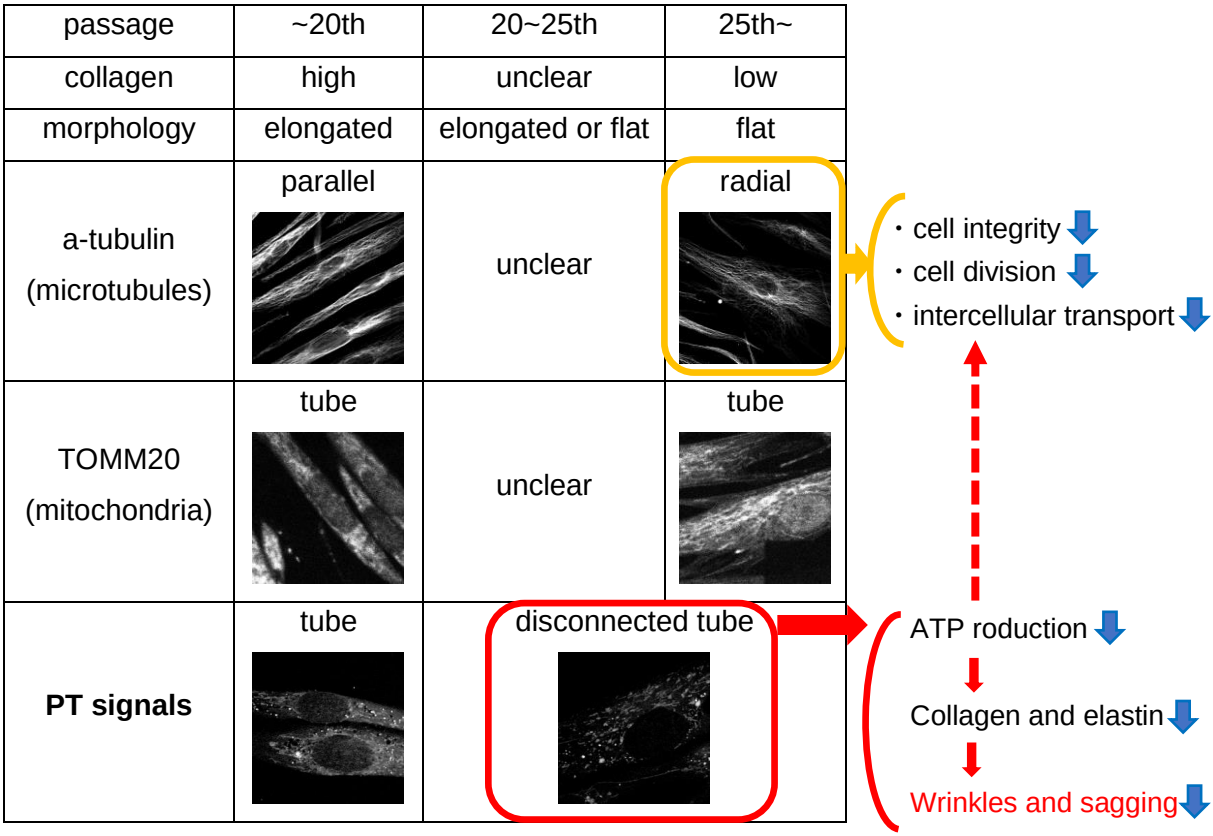

Figure 9. Relationships among number of passage and several indexes of related aging. PT signals of 20-25th were looked like disconnected tube, indicating that ATP production. Photothermal microscopy will be a significant index of anti-aging including wrinkles and sagging.

6. Reference

1. Fisher, G. J., Kang, S., Varani, J., Bata-Csorgo, Z., Wan, Y., Datta, S., Voorhees, J. Mechanisms of photoaging and chronological skin aging. (2002) Arch Dermatol Nov; 138(11): 1462-1470.
2. Bielajew, B. J., Hu, J. A., Athanasiou, K. A. Collagen: quantification, biomechanics and role of minor subtypes in cartilage. (2020) Nature Reviews Materials 5: 730-747.
3. Myllyharju, J., Kivirikko, K. I. Collagens, modifying enzymes and their mutations in humans, flies and worms. (2004) Trends Genet Jan; 20(1): 33-43.
Canty E. G., Kadler K. E. Procollagen trafficking, processing and fibrillogenesis. (2005) J Cell Sci 118, 1341–1353.
4. McCaughey, J., Stevenson, N. L., Cross, S., Stephens, D. J. ER-to-Golgi trafficking of procollagen in the absence of large carriers. (2019) J Cell Biol Mar 4; 218(3): 929-948.
5. Tanzer, M. L. Cross-linking of collagen. (1973) Science May 11; 180(4086): 561-566.
6. Short, K. R., Bigelow, M. L., Kahl, J., Singh, R., Coenen-Schimke, J., Raghavakaimal, S., Nair, K. S. Decline in skeletal muscle mitochondrial function with aging in humans. PNAS. (2005) 102(15):5618–5623.
7. Standard Operating Procedure. National Cancer Institute-Frederick. (2006) 13214: 1-9.
8. Rasband, W.S., ImageJ, U. S. National Institutes of Health, Bethesda, Maryland, USA, http://rsb.info.nih.gov/ij/, 1997-2007.
9. Miyazaki, J., Toumon, Y. Label-free imaging of mitochondria and lysosomes within living cells via simultaneous dual-pump photothermal microscopy. Biomedical Optics Express. (2019) 10(11): 5852-5861.
10. Desai, S. P., Bhatia, S. N., Toner, M., Irimia, D. Mitochondrial localization and the persistent migration of epithelial cancer cells. Biophys. J. (2013) 104: 2077–2088.